Nonenzymatic Template-Directed RNA Synthesis Inside Model Protocells

Katarzyna Adamala and Jack W. Szostak

Science **342**, 1098 (2013);
DOI: 10.1126/science.1241888

Science (print ISSN 0036-8075; online ISSN 1095-9203) is published weekly, except the last week in December, by the American Association for the Advancement of Science, 1200 New York Avenue NW, Washington, DC 20005.

16. M. Umetani *et al.*, *Nat. Med.* **13**, 1185–1192 (2007).
17. Materials and methods are available as supplementary materials on *Science* Online.
18. C. E. Connor *et al.*, *Cancer Res.* **61**, 2917–2922 (2001).
19. C. T. Guy, R. D. Cardiff, W. J. Muller, *Mol. Cell. Biol.* **12**, 954–961 (1992).
20. E. Y. Lin *et al.*, *Am. J. Pathol.* **163**, 2113–2126 (2003).
21. M. Hansson, E. Ellis, M. C. Hunt, G. Schmitz, A. Babiker, *Biochim. Biophys. Acta* **1593**, 283–289 (2003).
22. A. Sica *et al.*, *Semin. Cancer Biol.* **18**, 349–355 (2008).
23. M. A. Lyons, A. J. Brown, *Lipids* **36**, 701–711 (2001).
24. G. Llaverias *et al.*, *Am. J. Pathol.* **178**, 402–412 (2011).
25. N. Alikhani *et al.*, *Oncogene* **32**, 961–967 (2013).
26. R. Karuna *et al.*, *Atherosclerosis* **214**, 448–455 (2011).
27. P. M. Sullivan *et al.*, *J. Biol. Chem.* **272**, 17972–17980 (1997).

Acknowledgments: This work was funded by the NIH [grants K99CA172357 (E.R.N.) and R37DK048807 (D.P.M.)] and the U.S. Department of Defense (DOD) [grants BC085585 (E.R.N.) and DOD BC094960 (D.P.M.)]. The content of this paper is solely the responsibility of the authors and does not necessarily represent the official views of the NIH or DOD.

Expression profiling data on 27HC in MCF7 cells were uploaded to Gene Expression Omnibus (GEO) (accession no. GSE46924) and were part of a larger study (GEO accession no. GSE35428).

Supplementary Materials

www.sciencemag.org/content/342/6162/1094/suppl/DC1
Materials and Methods
Supplementary Text
Figs. S1 to S14
References (*28*–*33*)

13 June 2013; accepted 25 October 2013
10.1126/science.1241908

Nonenzymatic Template-Directed RNA Synthesis Inside Model Protocells

Katarzyna Adamala[1,2] and Jack W. Szostak[1]*

Efforts to recreate a prebiotically plausible protocell, in which RNA replication occurs within a fatty acid vesicle, have been stalled by the destabilizing effect of Mg^{2+} on fatty acid membranes. Here we report that the presence of citrate protects fatty acid membranes from the disruptive effects of high Mg^{2+} ion concentrations while allowing RNA copying to proceed, while also protecting single-stranded RNA from Mg^{2+}-catalyzed degradation. This combination of properties has allowed us to demonstrate the chemical copying of RNA templates inside fatty acid vesicles, which in turn allows for an increase in copying efficiency by bathing the vesicles in a continuously refreshed solution of activated nucleotides.

The RNA world hypothesis suggests that the primordial catalysts were ribozymes (*1*, *2*), whereas biophysical considerations suggest that the primordial replicating compartments were membranous vesicles composed of fatty acids and related amphiphiles (*3*, *4*). However, the conditions required for RNA replication chemistry and fatty acid vesicle integrity have appeared to be fundamentally incompatible (*5*) (fig. S1). Both ribozyme-catalyzed and nonenzymatic RNA copying reactions require high (50 to 200 mM) concentrations of Mg^{2+} (or other divalent) ions (*6*), but Mg^{2+} at such concentrations destroys vesicles by causing fatty acid precipitation.

We developed a screen for small molecules that protect oleate fatty acid vesicles from disruption by Mg^{2+}. We used two assays to monitor the leakage of either a small charged molecule (calcein) or a larger oligonucleotide, allowing us to distinguish between increased membrane permeability (faster calcein release with oligonucleotide retention) and generalized membrane disruption (rapid release of both calcein and the oligonucleotide) (figs. S2 to S4). We identified several chelators, including citrate, isocitrate, oxalate, nitrilotriacetic acid (NTA), and EDTA, that protect oleate vesicles in the presence of at least 10 mM Mg^{2+} (figs. S5 and S6). In the presence of chelated Mg^{2+}, oleate vesicles remained intact but exhibited a modest increase in the permeability of a small polar molecule (Fig. 1 and fig. S7) and an even smaller increase in the leakage of an oligonucleotide. In terms of vesicle stabilization, citrate was one of the most effective chelators of Mg^{2+}.

We also examined the stability of model protocell membranes made of myristoleic acid:glycerol monomyristoleate (2:1) and from the more prebiotically reasonable decanoic acid:decanol:glycerol monodecanoate (4:1:1). Citrate-chelated Mg^{2+} caused only a small amount of leakage from these vesicles, and the stabilizing effect of citrate was seen for both calcein and oligonucleotides (Fig. 1 and figs. S8 to S13).

We then asked whether these chelators were compatible with the Mg^{2+} catalysis of nonenzymatic template-directed RNA primer extension. We measured the rate at which an RNA primer was elongated when annealed to an oligonucleotide with a templating region of C nucleotides, in the presence of an excess of the activated G monomer guanosine 5′-phosphor(2-methyl)imidazolide (2MeImpG) (Fig. 2). We examined citric acid, EDTA, NTA, and a weakly stabilizing chelator (isocitric acid). In the presence of 50 mM unchelated Mg^{2+}, the primer-extension reaction proceeded at a rate of 1.4 $hour^{-1}$, compared to 0.03 $hour^{-1}$ in the absence of Mg^{2+} ions. The addition of four equivalents of EDTA or NTA resulted in complete abolition of Mg^{2+} catalysis (Fig. 2 and figs. S14 and S15), indicating that the Mg^{2+} in these samples is chelated in a fashion incompatible with promoting primer extension. In contrast, four equivalents of citrate only decreased the rate of primer extension to 0.67 $hour^{-1}$. For comparison, isocitric acid does not fully protect vesicles (figs. S16 and S17) but also does not affect the primer extension reaction.

To see whether citrate would allow nonenzymatic RNA copying to proceed within fatty acid vesicles, we encapsulated an RNA primer-template complex inside oleate vesicles, added Mg^{2+} and citrate, and removed unencapsulated RNA by size exclusion chromatography. We then added the activated G monomer 2MeImpG, heated the sample briefly to allow for rapid monomer permeation (*7*), and then incubated it at room temperature for times up to 24 hours to allow

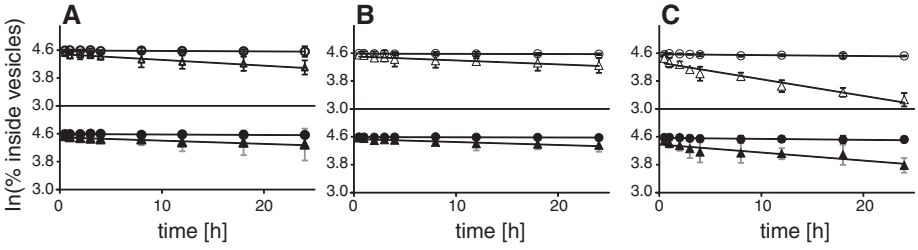

Fig. 1. Citrate stabilizes fatty acid vesicles in the presence of Mg^{2+} ions. Leakage of a small charged molecule (calcein, open symbols) and a larger nine-oligomer oligodeoxynucleotide (solid symbols) from fatty acid vesicles is shown. (**A**) Oleate vesicles; (**B**) myristoleate:glycerol monomyristoleate 2:1 vesicles; (**C**) decanoate:decanol:glycerol monodecanoate 4:1:1 vesicles. Circles, no $MgCl_2$, no citrate; triangles, 50 mM $MgCl_2$, 200 mM Na^+-citrate. The assay used to obtain these data is described in fig. S3. Lines are linear fits, coefficient of determination (R^2) ≥ 0.97. All experiments were repeated twice; error bars are mean ±2 SE.

[1]Howard Hughes Medical Institute, Department of Molecular Biology, and Center for Computational and Integrative Biology, Massachusetts General Hospital, Boston, MA 02114, USA. [2]Dipartimento di Biologia, Università degli Studi di Roma Tre, Rome, Italy.

*Corresponding author at Howard Hughes Medical Institute, Department of Molecular Biology, and Center for Computational and Integrative Biology, 7215 Simches Research Center, Massachusetts General Hospital, 185 Cambridge Street, Boston, MA 02114, USA. E-mail: szostak@molbio.mgh.harvard.edu

the monomer to take part in template-copying chemistry inside the vesicles. Analysis of the reaction products showed that after 24 hours of incubation, most of the primer had been extended by the addition of six G residues, with a smaller fraction extended to full length by the addition of a seventh G residue (Fig. 3). In parallel experiments with vesicles composed of mixtures of shorter-chain lipids, the brief heating step was not

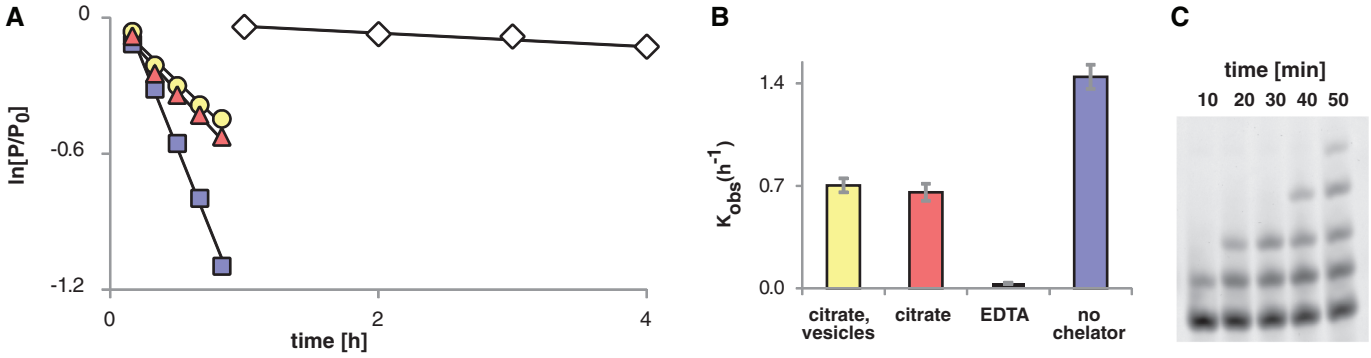

Fig. 2. The rate of RNA template-directed primer extension in the presence or absence of Mg^{2+} chelators and fatty acid vesicles. (**A**) Time courses of primer extension on a templating region of four C residues, expressed as a fraction of unextended primer remaining versus time. Squares, no chelators; triangles, 200 mM Na^+-citrate; circles, 200 mM Na^+-citrate and 100 mM oleate vesicles; diamonds, 200 mM EDTA. Lines are linear fits, $R^2 \geq 0.97$; the slope is k_{obs} ($hour^{-1}$). (**B**) Rates of primer extension under the indicated conditions; each kinetic experiment was performed in duplicate, and rates are determined as an average of the three separate runs. Error bars indicate SEM, $n = 3$ independent repetitions. (**C**) Typical polyacrylamide gel electrophoresis (PAGE) analysis of a template-directed primer extension experiment. Primer extension was carried out in the presence of 200 mM Na^+-citrate. For the gel analysis of the reactions used to obtain this data, see fig. S15.

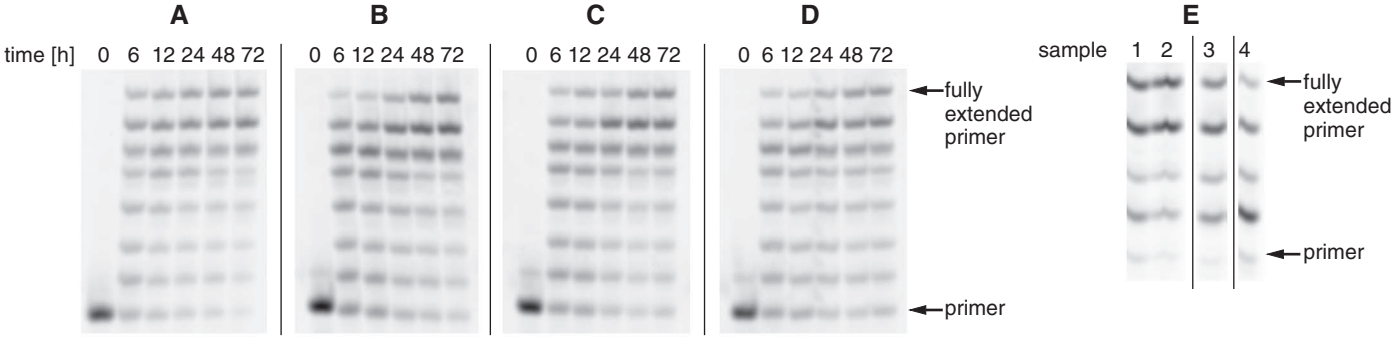

Fig. 3. RNA template copying inside model protocell vesicles. (**A** to **D**) Primer extension on a templating region of seven C residues. (A) Control reaction in solution; (B) inside oleate vesicles; (C) inside myristoleate:glycerol monomyristoleate 2:1 vesicles; (D) inside decanoate:decanol:glycerol monodecanoate 4:1:1 vesicles. (**E**) Extension of labeled RNA primer annealed to a mixed base template, templating region sequence GCCG. Sample 1, reaction inside myristoleate:glycerol monomyristoleate 2:1 vesicles; sample 2, reaction inside decanoate:decanol:glycerol monodecanoate 4:1:1 vesicles. Both sample 1 and 2 reactions were performed inside a liposome dialyzer (see the supplementary materials for the description of the liposome dialyzer) with a total of 13 buffer exchanges. Sample 3, control reaction in solution with daily addition of fresh portion of activated monomers, without removing the hydrolyzed monomers. Sample 4, control reaction in solution, without the addition of fresh monomer.

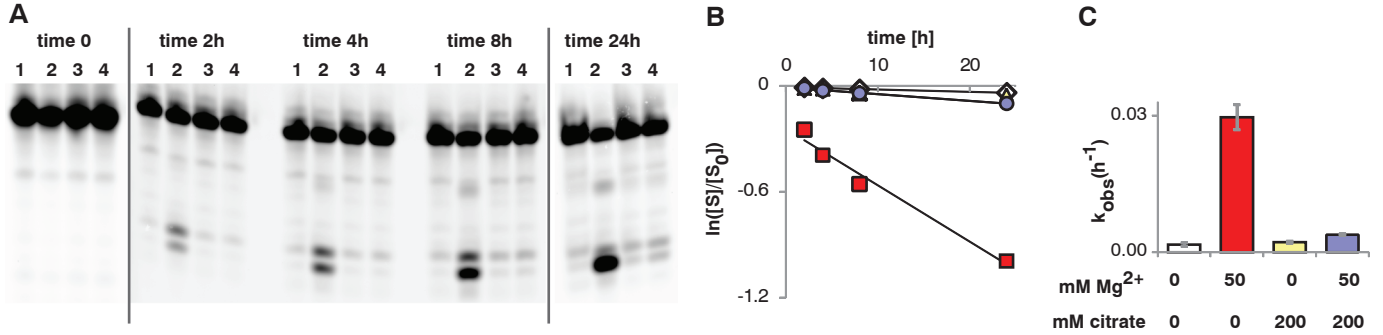

Fig. 4. Citrate protects RNA from Mg^{2+}-catalyzed degradation. (**A**) PAGE analysis of cleavage of a DNA oligonucleotide at the site of a single internal ribonucleotide, at indicated time points; lane 1, no Mg^{2+}, no citrate; lane 2, 50 mM Mg^{2+}, no citrate; lane 3, no Mg^{2+}, 200 mM citrate; lane 4, 50 mM Mg^{2+}, 200 mM citrate. (**B**) Quantitation of strand cleavage, expressed as a fraction of the intact substrate over total substrate versus time. Diamonds, no Mg^{2+}, no citrate; triangles, no Mg^{2+}, 200 mM citrate; circles, 50 mM Mg^{2+}, 200 mM citrate; squares, 50 mM Mg^{2+}, no citrate. Lines are linear fits, $R^2 \geq 0.97$. (**C**) Rates of strand cleavage at the *ribo* linkage with and without Mg^{2+} and citrate. Error bars indicate SEM, $n = 3$ independent repetitions.

necessary, because of the higher permeability of such membranes to nucleotide monomers. It is noteworthy that RNA primer extension occurred efficiently inside vesicles made of decanoic acid: decanol:glycerol monodecanoate (4:1:1) (Fig. 3), because short-chain saturated amphiphilic compounds are more prebiotically plausible than longer-chain unsaturated fatty acids such as oleate or myristoleate. When we encapsulated the RNA primer-template complex inside POPC vesicles, no primer extension was observed, because of the impermeability of phospholipid vesicles to the 2MeImpG monomer (even with a heat pulse) (fig. S18).

The efficiency of nonenzymatic RNA replication can be greatly enhanced by the periodic addition of fresh portions of activated monomer to a primer-extension reaction occurring on templates immobilized by covalent linkage to beads (*8*). We sought to reproduce this effect by mimicking the flow of an external solution of fresh monomers over vesicles, by periodic dialysis of model protocells against a solution of fresh activated monomers (see the supplementary materials for a description of the liposome reactor dialyzer). The control primer-extension reaction in solution shows that the yield of full-length primer-extension product from copying a GCCG template is very low, even if fresh monomers are added to the reaction periodically (Fig. 3E). In contrast, after repeated exchanges of external solution by dialysis, the proportion of full-length product was much greater (Fig. 3E).

The high thermal stability of the RNA duplex is a major problem for prebiotic RNA replication (*5*). Because Mg^{2+} greatly increases the melting temperature (T_m) of RNA duplexes, we asked whether the chelating properties of citrate would prevent the increase in the T_m of RNA duplexes caused by the presence of free Mg^{2+} ions. We observed a small but reproducible decrease in T_m in the presence of citrate when compared to samples containing unchelated Mg^{2+} (table S1 and figs. S19 and S20). For example, in the presence of 50 mM Mg^{2+} with four equivalents of citrate, the T_m of the RNA duplex was 71°C, whereas in the control sample without citrate the T_m was 75°C.

Citrate also stabilizes RNA by preventing the Mg^{2+} catalysis of RNA degradation. Incubating a 13-oligomer oligodeoxynucleotide with one *ribo* linkage at 75°C, with and without Mg^{2+} and citrate, results in significant strand cleavage at the site of the single *ribo* linkage. Four equivalents of citrate, relative to Mg^{2+}, abolished the Mg^{2+}-catalyzed degradation (Fig. 4). The observed rate constant (k_{obs}) for cleavage at the *ribo* linkage, at 75°C in the presence of 50 mM Mg^{2+} was 0.03 $hour^{-1}$, whereas in the presence of a fourfold excess of citrate, the rate decreased to 0.004 $hour^{-1}$.

The chelation of Mg^{2+} by citrate exhibits two protective effects in the context of model protocells: Protocell membranes based on fatty acids are protected from the disruption caused by the precipitation of fatty acids as Mg^{2+} salts, and single-stranded RNA oligonucleotides are protected from Mg^{2+}-catalyzed degradation. Based on the known affinity of citrate for Mg^{2+} (*9*, *10*), it is clear that the RNA synthesis observed in the presence of Mg^{2+} and citrate cannot be due to residual free Mg^{2+} (less than 1 mM) and must be due to catalysis by the Mg^{2+}-citrate complex. The crystal structure of Mg^{2+}-citrate (*11*) shows that the Mg^{2+} ion is coordinated by the hydroxyl and two carboxylates of citrate, so that three of the six coordination sites of octahedral Mg^{2+} are occupied by citrate, while the remaining three are free to coordinate with water or other ligands. The clear implication is that coordination of Mg^{2+} by at most three sites is sufficient for catalysis of template-directed RNA synthesis, but not for catalysis of RNA degradation or for the precipitation of fatty acids. In the absence of a prebiotic citrate synthesis pathway [but see (*12*) for a recent advance], it is of interest to consider prebiotically plausible alternatives to citrate that could potentially confer similar effects, such as short acidic peptides. Just such a peptide constitutes the heart of cellular RNA polymerases, where it binds and presents the catalytic Mg^{2+} ion in the active site of the enzyme.

References and Notes

1. W. Gilbert, *Nature* **319**, 618 (1986).
2. G. F. Joyce, *Nature* **338**, 217–224 (1989).
3. J. M. Gebicki, M. Hicks, *Nature* **243**, 232–234 (1973).
4. D. W. Deamer, J. P. Dworkin, *Top. Curr. Chem.* **259**, 1–27 (2005).
5. J. W. Szostak, The eightfold path to non-enzymatic RNA replication. *J. Sys. Chem.* **3:2** (2012).
6. J. C. Bowman, T. K. Lenz, N. V. Hud, L. D. Williams, *Curr. Opin. Struct. Biol.* **22**, 262–272 (2012).
7. S. S. Mansy, J. W. Szostak, *Proc. Natl. Acad. Sci. U.S.A.* **105**, 13351–13355 (2008).
8. C. Deck, M. Jauker, C. Richert, *Nat. Chem.* **3**, 603–608 (2011).
9. A. K. Covington, E. Y. Danish, *J. Solution Chem.* **38**, 1449–1462 (2009).
10. M. Walser, *J. Phys. Chem.* **65**, 159–161 (1961).
11. C. K. Johnson, *Acta Crystallogr.* **18**, 1004–1018 (1965).
12. C. Butch *et al.*, *J. Am. Chem. Soc.* **135**, 13440–13445 (2013).

Acknowledgments: We thank A. Engelhart, C. Hentrich, A. Larsen, N. Kamat, and A. Björkbom for discussions and help with manuscript preparation and A. Gifford for help with vesicle leakage experiments. This work was supported in part by NASA Exobiology grant NNX07AJ09G. J.W.S. is an investigator of the Howard Hughes Medical Institute. Raw data are presented in the supplementary materials. The instructions for assembling the Liposome Dialyzer are available at http://molbio.mgh.harvard.edu/szostakweb/.

Supplementary Materials

www.sciencemag.org/content/342/6162/1098/suppl/DC1
Materials and Methods
Supplementary Text
Figs. S1 to S21
Tables S1 to S3
Liposome Dialyzer Instructions
References (*13*–*15*)

13 June 2013; accepted 25 September 2013
10.1126/science.1241888

Primate Transcript and Protein Expression Levels Evolve Under Compensatory Selection Pressures

Zia Khan,[1]* Michael J. Ford,[2] Darren A. Cusanovich,[1] Amy Mitrano,[1] Jonathan K. Pritchard,[1,3]*† Yoav Gilad[1]*

Changes in gene regulation have likely played an important role in the evolution of primates. Differences in messenger RNA (mRNA) expression levels across primates have often been documented; however, it is not yet known to what extent measurements of divergence in mRNA levels reflect divergence in protein expression levels, which are probably more important in determining phenotypic differences. We used high-resolution, quantitative mass spectrometry to collect protein expression measurements from human, chimpanzee, and rhesus macaque lymphoblastoid cell lines and compared them to transcript expression data from the same samples. We found dozens of genes with significant expression differences between species at the mRNA level yet little or no difference in protein expression. Overall, our data suggest that protein expression levels evolve under stronger evolutionary constraint than mRNA levels.

Measurements of mRNA levels have revealed substantial differences across primate transcriptomes (*1*–*3*) and have led to the identification of putatively adaptive changes in transcript expression (*4*). Traditionally, measurements of divergence in mRNA levels are assumed to be good proxies for divergence in protein levels. However, there are numerous mechanisms by which protein expression may be regulated independently of mRNA levels (*5*, *6*). If transcript and protein expression levels are often uncoupled, mRNA levels may evolve under reduced constraint as changes at the transcript level could be buffered or compensated for at the

[1]Department of Human Genetics, University of Chicago, Chicago, IL 60637, USA. [2]MS Bioworks, LLC, 3950 Varsity Drive, Ann Arbor, MI 48108, USA. [3]Howard Hughes Medical Institute, University of Chicago, Chicago, IL 60637, USA.

*Corresponding author. E-mail: zia@uchicago.edu (Z.K.); pritch@stanford.edu (J.K.P); gilad@uchicago.edu (Y.G.)
†Present address: Departments of Genetics and Biology, Stanford University, Stanford, CA 94305, USA.